



University of Szeged

Faculty of Pharmacy

Institute of Pharmaceutical Technology and Regulatory Affairs

Head: Prof. Dr. Ildikó Csóka, Ph.D.

Summary of Ph.D. thesis

**DEVELOPMENT OF MELOXICAM CONTAINING CARRIER-FREE
“NANO-IN-MICRO” DRY POWDER INHALER SYSTEMS**

By

dr. Petra Party

Pharmacist

Supervisor:

Dr. habil. Rita Ambrus, Ph.D.

Szeged

2024

University of Szeged

Doctoral School of Pharmaceutical Sciences

Head: Prof. Dr. Judit Hohmann, D.Sc.

Educational program: Pharmaceutical technology and Regulatory Science

Head: Prof. Dr. Ildikó Csóla, Ph.D.

Institute of Pharmaceutical Technology and Regulatory Affairs

Supervisor: Dr. Rita Ambrus, Ph.D.

Dr. Petra Party

**DEVELOPMENT OF MELOXICAM CONTAINING CARRIER-FREE
“NANO-IN-MICRO” DRY POWDER INHALER SYSTEMS**

Complex Exam Committee:

- Head:** Prof. Dr. Piroska Szabó-Révész, D.Sc., University of Szeged,
Institute of Pharmaceutical Technology and Regulatory Affairs
- Members:** Dr. Gabriella Csóka, Ph.D., Meditop Pharmaceutical Ltd.
Pilisborosjenő
- Dr. Mária Budai-Szűcs, Ph.D., University of Szeged, Institute of
Pharmaceutical Technology and Regulatory Affairs

Reviewer Committee:

- Head:** Prof. Dr. István Szatmári, D.Sc. University of Szeged, Institute of
Pharmaceutical Chemistry
- Reviewers:** Prof. Dr. Noémi Csaba, Ph.D., University of Santiago de
Compostela, Department of Pharmacology, Pharmacy and
Pharmaceutical Technology
- Dr. Franciska Erdő Ph.D., Pázmány Péter Catholic University,
Faculty of Information Technology and Bionics
- Secretary:** Dr. Renáta Minorics, Ph.D., University of Szeged, Institute of
Pharmacodynamics and Biopharmacy
- Member:** Dr. Andrea Vasas, Ph.D., University of Szeged, Department of
Pharmacognosy

ABBREVIATIONS

A549 cells	Adenocarcinomic human alveolar basal epithelial cells	IL-6	Interleukin 6
		J	Flux
		K_p	Permeability coefficient
ACI	Andersen cascade impactor	LEU	L-leucine
		LPS	Lipopolysaccharide
API	Active pharmaceutical ingredient	MMAD	Mass median aerodynamic diameter
BCS	Biopharmaceutical Classification System	MX	Meloxicam
		NSAID	Non-steroidal anti-inflammatory drug
CF	Cystic fibrosis		
CI	Carr index	NSCLC	Non-small cell lung cancer
COPD	Chronic obstructive pulmonary disease		
		NTA	Nanoparticle tracking analysis
COVID-19	Coronavirus disease of 2019	PdI	Polydispersity index
		PM	Physical mixture
COX-2	Cyclooxygenase-2 enzyme	PSD	Particle size distribution
		PVA	Polyvinyl alcohol
D[0.1]	10% of the volume distribution is below this value	qPCR	Quantitative polymerase chain reaction
D[0.5]	50% of the volume distribution is below this value	RI	Refractive index
		S.D.	Standard deviation
D[0.9]	90% of the volume distribution is below this value	SEM	Scanning electron microscopy
DLS	Dynamic light scattering	SPD	Spray dried
DMSO	Dimethyl sulfoxide	SSA	Specific surface area
DPI	Dry powder inhaler	T_g	Glass transition temperature
DSC	Differential scanning calorimetry		
		X_c	Degree of crystallinity
EF	Emitted fraction	XRPD	X-ray powder diffraction
ELISA	Enzyme-linked immunosorbent assay	Z-average	Average hydrodynamic diameter
FPF	Fine particle fraction	ζ pot.	Zeta potential
HR	Hausner ratio	ρ_b	Bulk density
ICH	the International Council for Harmonization (ICH	ρ_t	Tapped density

1. Introduction

The burden of chronic lung diseases has increased dramatically over the past decades. In terms of prevalence, the five most prominent lung diseases are asthma, tuberculosis, chronic obstructive pulmonary disease (COPD), lung cancer and pneumonia caused by various infections. Local treatment of the conditions compared to oral or parenteral drug delivery could be more efficient with better patient compliance.

Among the pulmonary drug delivery systems, the application of dry powder inhalers (DPIs) continues to grow in therapy due to their outstanding stability, ease of use and low production costs. Advantages compared to propellant aerosols are that the inhaled air stream delivers the drug to the airways, which can significantly reduce greenhouse gas emissions. Compared to conventional carrier-based DPIs, carrier-free DPIs are more effective, because the active pharmaceutical ingredient (API) creates a complex system with additives. Due to their special morphology, structure, and better aerodynamic properties, even low respiratory function is enough for proper lung deposition.

The majority of APIs used today are poorly water-soluble. Nanosized drugs can provide higher bioavailability due to their smaller particle size and larger specific surface. The various size reduction methods include bottom-up and top-down approaches. Water-solubility can be improved by applying particle engineering techniques that also enable new, alternative administration routes.

Although pulmonary therapy would benefit from the use of nanoparticles, there is no commercially available formulation yet. The main challenge is that the required aerodynamic particle size should be between 1-5 μm . For this, the “nano-in-micro” structure could be a solution, having the advantages of nanosized drugs while providing adequate aerodynamic properties. The combination of wet milling, as a top-down particle size reduction method, and spray drying, as a bottom-up technology, could be suitable for their preparation. These systems deposit deeper into the respiratory tract compared to the conventional formulations, while overcoming its elimination mechanisms.

It is difficult in pharmaceutical technology to find organic solvent-free, scalable, cost-effective and time-saving techniques that are suitable for the preparation of the “nano-in-micro” DPIs. This thesis reports the development of DPIs containing the non-steroidal anti-inflammatory agent (NSAID) meloxicam (MX) using a combined preparation technique with the aim of effective pulmonary delivery.

2. Aim of the work

This Ph.D. work aimed to develop innovative MX containing carrier-free “nano-in-micro” DPIs for pulmonary delivery. Efficiency in the lungs is based on the appropriate particle properties, aerodynamic diameter and proper drug release. The research work was planned considering the development requirements [1,2] according to the following steps:

- I. To review the literature on basic properties, suitable excipients, preparation techniques, and mechanism of action of “nano-in-micro” DPI systems and identify the available NSAID containing DPI formulations.
- II. To develop the formulation strategy and composition without organic solvent to achieve MX nanosuspension *via* wet milling, with particle size below 200 nm.
- III. To optimize the preparation method and composition of MX-containing “nano-in-micro” particles, with proper particle size, narrow size distribution and spherical morphology, using mini and nano spray drying devices. The DPIs were designed to have a particle size in the 2–5 μm range and particles smaller than 2 μm respectively. A comparison study was conducted to establish the advantages and disadvantages of the two spray drying methods, while the performance of the selected additives was observed during the investigations.
- IV. To determine the *in vitro* and *in silico* aerodynamic properties of DPIs at different flow rates using the Andersen cascade impactor (ACI) and the stochastic lung model to prove the proper lung deposition.
- V. To describe the pulmonary applicability of the formulation, *in vitro* drug release study and *in vitro* permeability study were performed under pulmonary conditions. In addition, *in vitro* cytotoxicity and anti-inflammatory tests were implemented.
- VI. Lastly, our aim was to test the physical stability of the DPI in a long-term study according to the International Council for Harmonization (ICH) Q1A guideline.

In overall, the goal was to provide novel MX containing “nano-in-micro” DPIs for the treatment of respiratory diseases by implementing the therapeutic advantages of nanoparticles and an alternative delivery route. In addition to the application of modern particle engineering techniques, the development of a comprehensive investigation protocol for DPIs was also aimed. The formulation strategy could be easily adapted to existing APIs, therefore opening up modified therapeutic protocols and advanced treatments, which could lead to long-term cost reduction in chronic treatments.

3. Materials

3.1. Active pharmaceutical ingredient

The NSAID MX (International Union of Pure and Applied Chemistry, IUPAC name: 4-hydroxy-2-methyl-N-(5-methyl-1,3-thiazol-2-yl)-1,1-dioxo-1λ6,2-benzothiazine-3-carboxamide, was used as the API (Egis Pharmaceuticals PLC., Budapest, Hungary), which is a poorly water-soluble drug (in water, 7.15 mg/l at 25 °C).

3.2. Excipients

Poly-vinyl-alcohol 4–98 (PVA, M_w ~27.000 g/mol, Sigma-Aldrich, St. Louis, MO, USA) was used to stabilize the samples. L-leucine (LEU, M_w : 131.17 g/mol, AppliChem GmbH, Darmstadt, Germany) was applied to enhance dispersity.

4. Preparation methods of the “nano-in-micro” DPI systems

4.1. Production of the nanosuspension by wet milling

The MX containing nanosuspension was prepared as follows: 2.00 g of MX and 18.00 g of 2.5% (w/w%) PVA solution were added to a planetary ball mill (Retsch PM 100; Retsch GmbH, Haan, Germany). The following conditions were used: 20.00 g of zirconium-dioxide (ZrO_2) beads ($d = 0.3$ mm), 500 rpm, 60 min. Before spray drying the nanosuspension was diluted with purified water to 500 ml.

4.2. DPI formulation by spray drying

4.2.1. Mini spray drying method

Three compositions were prepared by adding various amounts of LEU to the MX suspension (Table 1.). Solid particles were produced using a spray dryer equipped with a two-fluid nozzle of 0.7 mm (Büchi Mini Spray Dryer B-191, Büchi, Flawil, Switzerland). The drying properties were as follows: inlet temperature: 165 °C, outlet temperature: 100 °C, aspirator capacity: 85%, airflow rate 500 l/h and feed pump rate: 10%.

4.2.2. Nano spray drying method

Three similar compositions were formulated from the MX nanosuspension by adding different amounts of LEU (Table 1). The inhalable powders were produced with a Büchi Nano Spray Dryer (Büchi Nano Spray Dryer B-90 HP, Büchi, Flawil, Switzerland). To produce particles under 2 μ m the device was equipped with a small nebulizer (hole size: 4 μ m). The drying parameters were derived from the preliminary data: inlet temperature: 80 °C, aspirator capacity: 100%, airflow rate: 120 ml/min, pump rate: 20%.

4.3. Preparation of the physical mixtures

A physical mixture (PM) was created from the raw materials to observe the effect of the excipients. The composition of the PM was equal to the SPD samples (Table 1.). The API content of the final powders was determined (see Section 6.5.1.).

Table 1. Composition of the SPD samples and the PMs, yield of the drying methods and API contents.

Sample name	MX (g)	PVA (g)	LEU (g)	Yield (%)	API content (%)
mini[MX1_PVA_LEU0]	2.00	0.45	0.00	45.41 ± 5.10	93.81 ± 2.99
mini[MX1_PVA_LEU0.5]	2.00	0.45	1.00	57.56 ± 1.36	55.48 ± 0.78
mini[MX1_PVA_LEU1]	2.00	0.45	2.00	58.43 ± 6.36	51.46 ± 2.99
nano[MX1_PVA_LEU0]	2.00	0.45	0.00	61.44 ± 3.34	72.50 ± 3.55
nano[MX1_PVA_LEU0.5]	2.00	0.45	1.00	63.29 ± 2.38	51.26 ± 3.19
nano[MX1_PVA_LEU1]	2.00	0.45	2.00	62.44 ± 5.86	42.65 ± 1.33
pm[MX1_PVA_LEU0]	2.00	0.45	0.00	-	81.63
pm[MX1_PVA_LEU0.5]	2.00	0.45	1.00	-	57.97
pm[MX1_PVA_LEU1]	2.00	0.45	2.00	-	44.94

5. Characterization of the nanosuspension

5.1. Particle size analysis

5.1.1. Laser diffraction based particle size measurement

The particle size, PSD, and specific surface area (SSA) of the nanosuspension were determined by laser diffraction (Mastersizer Scirocco 2000, Malvern Instruments Ltd., Worcestershire, UK). The refractive index (RI) of the MX was set to 1.720. The suspension was measured three times in water with stirring at 2000 rpm, using the wet dispersion unit.

5.1.2. Dynamic light scattering investigations

The average hydrodynamic diameter (Z-average), polydispersity index (PdI), and zeta potential (ζ potential) were analyzed via dynamic light scattering (DLS) using a Zetasizer Nano ZS (Malvern Instruments, Worcestershire, UK). The suspension was diluted in purified water and measured at 25 °C in folded capillary cells. The RI of MX was adjusted to 1.720. Measurements were made in triplicate.

5.1.3. Nanoparticle tracking analysis

The NanoSight NS 3000 device (Malvern Instruments, Worcestershire, UK) for nanoparticle tracking analysis (NTA) was used to obtain high-resolution particle size information. The instrument was equipped with a 565 nm laser, a high sensitivity sCMOS camera and a syringe pump. The MX suspension was diluted 1000 times and loaded into the device using a syringe pump speed of 50. The experiment videos were analyzed using NTA 3.4 Build 3.4.4 after capture in script control mode (3 videos of 30 s per measurement). A total of 1500 frames per sample were examined.

6. Solid phase characterization

6.1. Particle size analysis

6.1.1. Laser diffraction based particle size measurement

Laser diffraction was applied to determine the particle size, PSD and SSA of the SPD samples. The dry dispersion unit was used. The dispersion air pressure was set to 3.0 bar and a vibration feed was applied. The RI was set to 1.720. Each sample was measured three times. PSD was characterized by the values of D[0.1] (10% of the volume distribution is below this value), D[0.5] (50% of the volume distribution is below this value), and D[0.9] (90% of the volume distribution is below this value), (Equation 1.). The SSA was derived from the PSD data under the assumption of spherical particles.

$$\text{Span} = \frac{D[0.9]-D[0.1]}{D[0.5]} \quad (1)$$

6.1.2. Dynamic light scattering analysis

The Z-average, PdI, and ζ potential were analyzed *via* DLS. The SPD formulations were suspended in purified water and measured at 25 °C in folded capillary cells. The RI of MX was set to 1.720. Each measurement was carried out in triplicate.

6.2. Morphology investigation

The shape of the particles was analyzed using scanning electron microscopy (SEM, Hitachi S4700; Hitachi Ltd., Tokyo, Japan). The investigation conditions were the following: 10 kV high voltage, 10 mA amperage, and 1.3–13.1 mPa air pressure. A high vacuum evaporator and argon atmosphere were applied to make the sputter-coated samples conductive with gold-palladium (Bio-Rad SC 502; VG Microtech, Uckfield, UK).

6.3. Density and powder flow measurement

The bulk and tapped densities of the formulations were measured using a tap density tester (ETD-1020x, Electrolab, Mumbai, India). A cylinder was filled with 1.5-2.0 cm³ of powders to calculate the bulk density (ρ_b). It was tapped 1000 times. The tapped density (ρ_t) was calculated compared to the volume of the powder before and after the taps. The measurements were performed three times. The Hausner ratio (HR) and Carr index (CI) values of the samples were evaluated from the bulk density and the tapped density (Equation 2., 3.).

$$\text{HR} = \frac{\rho_t}{\rho_b} \quad (2)$$

$$\text{CI} = \frac{(\rho_t - \rho_b)}{\rho_t} * 100 \quad (3)$$

6.4. Determination of the crystallinity

6.4.1. Thermoanalytical measurement

Differential scanning calorimetry (DSC) measurements were performed with a Mettler Toledo DSC 821e thermal analysis system with the STARE thermal analysis program V9.1 (Mettler Inc., Schwerzenbach, Switzerland). The samples were heated to 300 °C at a rate of 10 °C/min while maintaining a steady flow of argon at a rate of 10 l/h.

6.4.2. Analysis of the crystalline structure

The crystalline structure was investigated using X-ray powder diffraction (XRPD). The Bruker D8 advance diffractometer and the VANTEC-1 detector (Bruker AXS GmbH, Karlsruhe, Germany) were used with Cu K λ I radiation. Scanning was performed at a uniform voltage of 40 kV and a current of 40 mA from 3° to 40°, scanning time constant was 0.1°/min, angular step was 0.01°. The DIFFRACplus EVA program was used for the evaluation. The degree of crystallinity (X_c) were determined (Equation 4.). A means the area under the curve: The PM were considered 100% crystalline.

$$X_c = \frac{A_{crystalline}}{A_{crystalline} + A_{amorphous}} * 100 \quad (4)$$

6.5. *In vitro* and *in silico* aerodynamic characterization of the DPI systems

6.5.1. Andersen cascade impactor measurement

The aerosolization properties of the SPD formulations were evaluated *in vitro*, using an Andersen cascade impactor (ACI, Copley Scientific Ltd., Nottingham, UK). The inhalation flow rate was set at 28.3 l/min and 60 l/min (High-capacity pump model HCP5, Critical flow controller model TPK, Copley Scientific Ltd., Nottingham, UK). The inhalation time was 4 s. The Breezhaler[®] single-dose device (Novartis International AG, Basel, Switzerland) was applied. Transparent size 3 gelatin capsules (Capsugel, Bornem, Belgium) were filled with the powders, containing 1.5 mg of MX. The API contents (Table 1.) of the different DPIs were determined by solving 1 mg of powder in 25 ml of methanol and pH 7.4 phosphate buffer (60+40 V/V%) and analyzed by UV/Vis spectrophotometry at a wavelength of 362 nm. To simulate the pulmonary adhesive conditions, the collection plates were coated with a mixture of span 85 and cyclohexane (1 + 99 w/w%). After the measurement, the device, capsules, induction port, plates and the filter (A/E glass fiber filter, Pall Corporation, NY, USA) were washed with methanol and pH 7.4 phosphate buffer (60+40 V/V%) to dissolve the deposited amount of MX. The API was quantified by UV/Vis spectrophotometry. Aerodynamic properties were evaluated using Inhalytix[™]

software (Copley Scientific Ltd., Nottingham, UK). The fine particle fraction (FPF) and mass median aerodynamic diameter (MMAD) values were determined. FPF is defined as the percentage of mass of the particles containing of API with an MMAD of less than 5 μm divided by the emitted dose of the formulations. The emitted fraction (EF) was calculated, which is the released fraction from the device.

6.5.2. *In silico aerodynamic characterization*

The *in silico* simulations were performed using the stochastic lung model, which tracks the inhaled particles until their deposition or exhalation and computes the fraction of the particles deposited in each anatomical part of the airways. In our work, the aerodynamic PSD of the samples measured by the ACI served as input for the numerical model of airway deposition. The inhalation parameters corresponded to the inhalation of a COPD patient through Breezhaler®, whose inhaled volume ($IV = 1.7 \text{ l}$) and inhalation time ($t_{\text{in}} = 3.2 \text{ s}$) corresponded to the best flow rate of the impactor measurements. Two different (5 s and 10 s) breath holding times were used. The computational deposition model was validated in earlier works. The test was carried out in cooperation with the Center for Energy Research of Hungarian Academy of Sciences.

6.6. ***In vitro investigations of the pulmonary dosage form***

6.6.1. *In vitro dissolution test using the conventional paddle method*

Currently, there are no regulatory requirements for the *in vitro* dissolution testing of inhaled products. A modified paddle method (Hanson SR8 Plus, Teledyne Hanson Research, Chatsworth, CA, USA) of the European Pharmacopeia was used to define the release of MX from the dosage form. The samples contained 1.5 mg of MX, which is the tenth of the highest oral dose of MX and the estimated dose of MX for pulmonary delivery. The estimated value of the lung lining fluid is between 10 and 70 ml. Considering the limitation of the dissolution setup, 50 ml of the previously mentioned simulated lung medium was applied. The paddle was rotated at 100 rpm and the measurement was performed up to 60 min at 37 °C. Samples of 5 ml were taken after 5, 10, 15, 30, and 60 min. The medium was replenished in all cases. After filtration (pore size: 0.45 μm , Millex-HV syringe-driven filter unit, Millipore Corporation, Bedford, MA, USA), the dissolved quantity of MX was determined spectrophotometrically at a wavelength of 362 nm. The measurement was performed three times.

6.6.2. *In vitro* permeability investigation

A 3D printed horizontal diffusion cell was used to investigate the *in vitro* permeability of the samples. 9 ml of artificial lung medium was used as the donor phase. The acceptor phase was 9 ml of phosphate buffer (pH = 7.4), simulating the circumstances of the lung epithelium. Between the two phases, a cellulose membrane (RC 55 Whatman™ GE Healthcare Life Sciences, Buckinghamshire, UK) was applied, which was impregnated with isopropyl myristate. The pore size of the membrane was 0.5 μm, its thickness was 0.75 μm. The diffusion surface was 0.785 cm². The rotation of the stirring bar was set to 300 rpm. The temperature was set at 37 °C. Samples containing 1.5 mg of MX were investigated. The amount of API diffused to the acceptor phase was determined at a wavelength of 362 nm, for 60 minutes with a spectrophotometric sonda (FDP-7UV200-VAR, Avaspec-ULS2048-USB2, Avantes, Apeldoorn, The Netherlands). Three parallel measurements were made. The flux (J) of MX was calculated from the quantity of MX, which permeated through the membrane (m), divided by the surface of the membrane insert (A_m) and the duration time (t) (Equation 6.). The permeability coefficient (K_p) was determined as flux and MX concentration in the donor phase [μg/cm³] (Equation. 7.).

$$J = \frac{m}{A_m \cdot t} \quad (6)$$

$$K_p = \frac{J}{C_d} \quad (7)$$

6.6.3. *In vitro* cell line investigations

6.6.3.1. Cytotoxicity measurement

The SPD samples were dissolved in dimethyl sulfoxide (DMSO, VWR Chemicals, Leuven, Belgium), a concentration of 0.1 mg/ml was applied. This concentration of MX is adequate for pulmonary administration. Further diluted concentrations were also tested. Mitochondrial activity as a measure of cell viability was performed using MTT (3-(4,5-dimethylthiazol-2-yl)-2,5-diphenyltetrazolium bromide) assay in 96-well cell culture microplates using A549 (adenocarcinomic human alveolar basal epithelial cells, ATCC). The cells were treated with either MX or nano SPD samples. The cytotoxicity was determined by measuring the optical density (OD) at 550 nm with an EZ READ 400 ELISA reader (Biochrom, Cambridge, UK). The assay was replicated four times for each concentration. Cell viability was concluded on the following Equation 8.

$$\text{Cell viability} = 100 - \frac{(OD_{\text{sample}} - OD_{\text{medium control}})}{(OD_{\text{control}} - OD_{\text{medium control}})} \times 100 \quad (8)$$

6.6.3.2. Measurement of the anti-inflammatory effect

Cells were propagated in minimum essential medium with Earle's salt (Sigma, St. Louis, MO, USA) and were supplemented with 25 µg/ml gentamycin, 10 % of fetal calf serum, 0.5 % w_t/vol of glucose, 0.3 mg/ml of l-glutamine and 4 mM HEPES. A549 cells were seeded in 6-well plates at a density of 1 x 10⁶ cells/well and treated with 0.1 mg/ml of MX or DPI formulations and 5 µg/ml of LPS or only 5 µg/ml of LPS or left untreated, then the cells were incubated for 48 h at 37 °C. After the treatment, ribonucleic acid (RNA) was extracted using the TRI reagent (Sigma-Aldrich, St. Louis, MS, USA). Subsequently, 0.1 µg of mRNA was reverse transcribed using Maxima reverse transcriptase using oligo(dT) primers (ThermoFisher Scientific, Waltham, MA, USA). Quantitative polymerase chain reaction (qPCR) was performed using a Bio-Rad CFX96 real-time system with the 5x HOT FIREPol[®] EvaGreen[®] qPCR Supermix (Solis BioDyne, Tartu, Estonia) and the following pairs of human-specific primers: interleukin-6 (IL-6) and Actb (actin beta). Threshold cycles (Ct) were determined for IL-6 and Actb, and the relative gene expression was calculated *via* the 2⁻($\Delta\Delta$ Ct) method. After 48 h of treatment, the supernatant of the cells was collected and a sandwich human IL-6 enzyme-linked immunosorbent assay ELISA kits Legend Max[™] (BioLegend, San Diego, CA, USA) was used to determine the IL-6 concentration. The plates were analyzed using the Biochrom Anthos 2010 microplate reader (Biochrom, Cambridge, UK). Samples were assayed in duplicate. The *in vitro* cell line tests were performed with the help of the Department of Medical Microbiology, University of Szeged.

6.7. Stability test

The stability of the nano[MX1_PVA_LEU1] sample was investigated. The results could also be extended to the other formulations, due to their similar composition. The stability test was performed at 25 ± 2 °C with 50 ± 5% relative humidity to mimic the room conditions in a desiccator. The samples were taken and measured after 1 day, 6 months and 12 months.

6.8. Statistical analysis

All the described data indicate the standard deviation (± SD) of three parallel measurements (n = 3). Statistical analysis was performed using Student's t test and one-way analysis of variance (ANOVA) using GraphPad Prism 8.0.1. software (GraphPad Software, CA, USA). P-values < 0.05 indicated statistically significant differences.

7. Result of the characterization of the nanosuspension

7.1. Particle size analysis

7.1.1. Results of the laser diffraction based particle size distribution

The initial diameter of the API was in the micrometric size range ($D[0.5] = 9.91 \pm 0.37 \mu\text{m}$), which was successfully reduced by wet milling to $D[0.5] = 137.70 \pm 4.97 \text{ nm}$. SSA increased from $1.09 \pm 0.03 \text{ m}^2/\text{g}$ to $43.65 \pm 5.32 \text{ m}^2/\text{g}$. PVA coated the MX particles, which inhibited particle aggregation during size reduction.

7.1.2. Outcomes of dynamic light scattering investigation

The DLS test showed that the Z-average of the suspension was $359.75 \pm 12 \text{ nm}$ and the PdI was 0.34 ± 0.06 . In addition, it proved that the diameter of MX was reduced under 500 nm. Therefore, the drug could avoid the uptake by alveolar macrophages. The ζ potential was -23.70 ± 0.85 , demonstrating a stable suspension.

7.1.3. Results of the nanoparticle tracking analysis

NTA simultaneously detects large and small particles, resulting in a more precise particle distribution, than DLS. According to NTA, $D[0.5]$ of the MX nanosuspension was $124.90 \pm 8.60 \text{ nm}$ and PSD was monodisperse (Figure 1.).

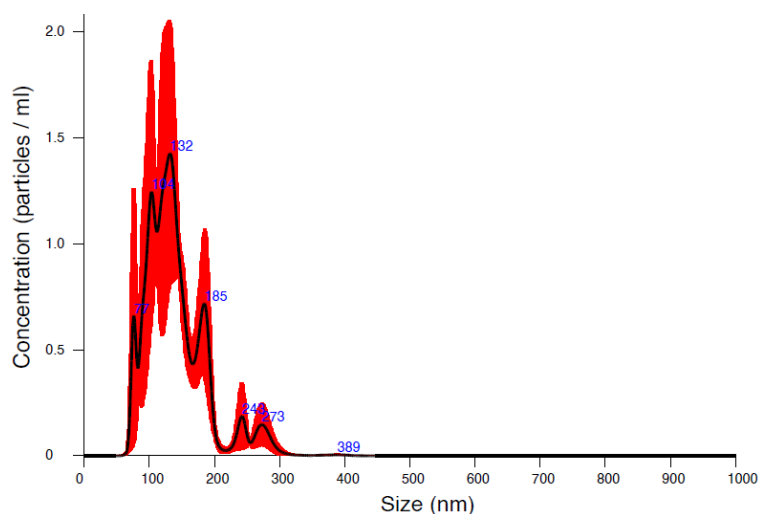


Figure 1. The particle size result of the suspension according to the NTA.

8. Results of the solid phase characterization

8.1. Particle size analysis

8.1.1. Results of the laser diffraction based particle size distribution

After solidification, the size of the particles was applicable for pulmonary delivery, since the $D[0.5]$ values were in the 1-5 μm range in all cases (Table 2.). The geometric diameter of the mini SPD samples was between 3.2-4.4 μm . After nano spray drying, the

D[0.5] values of the samples were between 1–1.5 μm . The results met the initial aim, which was to produce particles above and below 2 μm using the two different spray drying techniques. The incorporation of LEU increased the geometric size of the SPD particles, leading to a decrease in SSA. The reason behind this is that the particle-particle interaction forced to alter the size of the particle. The higher the Span value, the broader is the distribution. PSD was monodisperse (Span < 2.0) in the case of mini SPD and LEU containing nano SPD products, which is important for accurate doses.

Table 2. The particle size, Span and SSA values of the DPIs.

Sample name	D[0.5] (μm)	Span	SSA (m^2/g)
mini[MX1_PVA_LEU0]	3.19 ± 0.02	1.56 ± 0.07	2.22 ± 0.03
mini[MX1_PVA_LEU0.5]	3.80 ± 0.01	1.46 ± 0.00	1.88 ± 0.02
mini[MX1_PVA_LEU1]	4.40 ± 0.03	1.58 ± 0.08	1.71 ± 0.05
nano[MX1_PVA_LEU0]	1.17 ± 0.00	5.42 ± 1.49	6.60 ± 0.03
nano[MX1_PVA_LEU0.5]	1.31 ± 0.04	1.68 ± 0.30	5.19 ± 0.06
nano[MX1_PVA_LEU1]	1.43 ± 0.09	1.59 ± 0.12	4.39 ± 0.01

8.1.2. Outcomes of the dynamic light scattering investigation

Table 3. showed the outcomes of the DLS investigation. According to the results, the mini SPD samples will disintegrate slower than the nano SPD particles, due to the larger particle size. The inhomogeneous distribution was shown by the relatively high PDI results (PDI > 0.3). However, it was not considered a problem if it does not negatively affect the drug release. All systems were more degradable and less retentive in the airways due to the negative ζ potential values of the products.

Table 3. Z average, PDI and ζ potential of DPIs.

Sample name	Z average (nm)	PDI	ζ potential (mV)
mini[MX1_PVA_LEU0]	1852.00 ± 126	0.552 ± 0.056	-2.15 ± 0.25
mini[MX1_PVA_LEU0.5]	1292.00 ± 231	0.653 ± 0.065	-18.63 ± 2.06
mini[MX1_PVA_LEU1]	1386.00 ± 142	0.706 ± 0.074	-23.83 ± 1.19
nano[MX1_PVA_LEU0]	676.70 ± 47	0.543 ± 0.055	-21.35 ± 5.27
nano[MX1_PVA_LEU0.5]	743.25 ± 27	0.502 ± 0.074	-23.30 ± 2.74
nano[MX1_PVA_LEU1]	526.90 ± 20	0.381 ± 0.031	-24.50 ± 1.47

8.2. Findings of the morphology investigation

On the SEM images (Figure 2.) of the DPIs, the size differences between the different batches can be easily seen. A nearly spherical shape was observed, which was the result of the optimized spray drying methods. The spherical form met the requirements of DPIs. PVA prevented the aggregation of the particles because it created a hydrophilic layer around the drug particles. When LEU was present in the systems, preferable wrinkled

particles were established and the spherical morphology shifted to a shell-shaped appearance. The rough surface was formed as the rapidly drying core crumpled. LEU developed a crystalline layer, which reduced surface energy while improving surface rugosity. Therefore, LEU can reduce the adhesion between particles and the attachment to the capsule, resulting in higher EF and FPF values. The samples demonstrated an internal hollow structure, reflecting a low density. LEU enrichment can also result in moisture protection, therefore improving their physical storage stability.

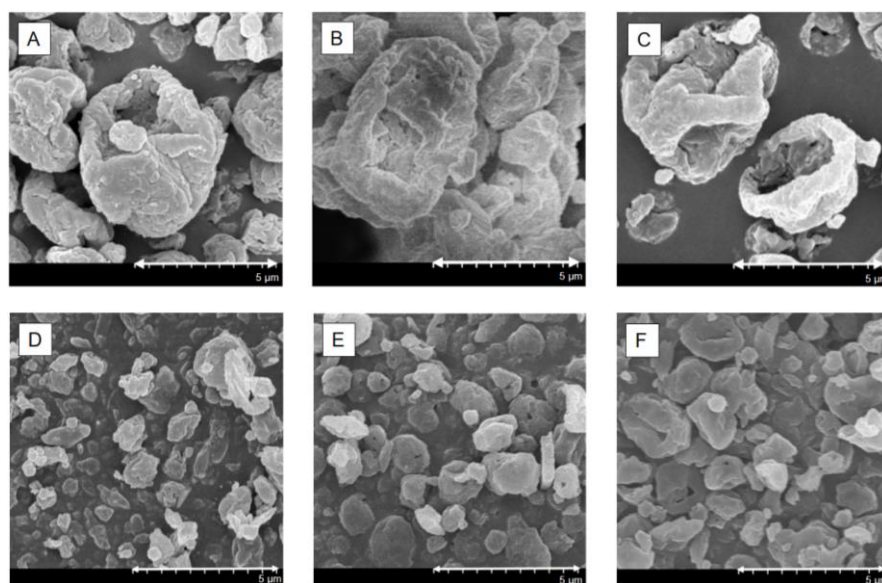


Figure 2. SEM pictures of the SPD samples: A: mini[MX1_PVA_LEU0], B: mini[MX1_PVA_LEU0.5], C: mini [MX1_PVA_LEU1], D: nano[MX1_PVA_LEU0], E: nano[MX1_PVA_LEU0.5], F: nano[MX1_PVA_LEU1].

8.3. Results of the density and powder flow test

The ρ_t of the products was lower than or around 0.3 g/cm^3 . The density of the commercially available DPIs is approximately 1 g/cm^3 , therefore, the samples can be considered as low-density formulations. Favorably, the lower the ρ_t is, the higher the FPF is. The application of a larger amount of LEU was reduced the ρ_b , therefore improved powder dispersibility. The HR and CI (Table 4.) were similar to other carrier-free formulations. The HR and CI values indicated powder flow, which is also responsible for aerosolization.

Table 4. Density, HR and CI results of the DPIs.

Sample name	$\rho_b(\text{g/cm}^3)$	$\rho_t(\text{g/cm}^3)$	HR	CI
mini[MX1_PVA_LEU0]	0.18 ± 0.02	0.26 ± 0.00	1.49 ± 0.05	32.39 ± 7.23
mini[MX1_PVA_LEU0.5]	0.16 ± 0.01	0.27 ± 0.00	1.76 ± 0.08	43.09 ± 2.70
mini[MX1_PVA_LEU1]	0.15 ± 0.01	0.20 ± 0.01	1.40 ± 0.21	27.65 ± 10.8
nano[MX1_PVA_LEU0]	0.22 ± 0.01	0.31 ± 0.01	1.33 ± 0.09	27.27 ± 4.55
nano[MX1_PVA_LEU0.5]	0.22 ± 0.01	0.32 ± 0.02	1.43 ± 0.10	30.00 ± 5.00
nano[MX1_PVA_LEU1]	0.21 ± 0.00	0.32 ± 0.01	1.50 ± 0.08	33.33 ± 3.33

8.4. Analysis of the crystallinity

8.4.1. Results of the thermoanalytical measurement

DSC was employed to investigate the MX melting process (Figure 3.). The raw MX showed a sharp endothermic peak at 264.03 °C, reflecting its melting point and crystallinity. After the preparation methods, the curves showed broader endothermic peaks of MX, indicating a decrease in their crystallinity. The residual MX crystals were melted at a lower temperature than the raw MX due to the smaller particle size and amorphization. This was promoted by PVA, which has a glass transition temperature (T_g) value at 85 °C.

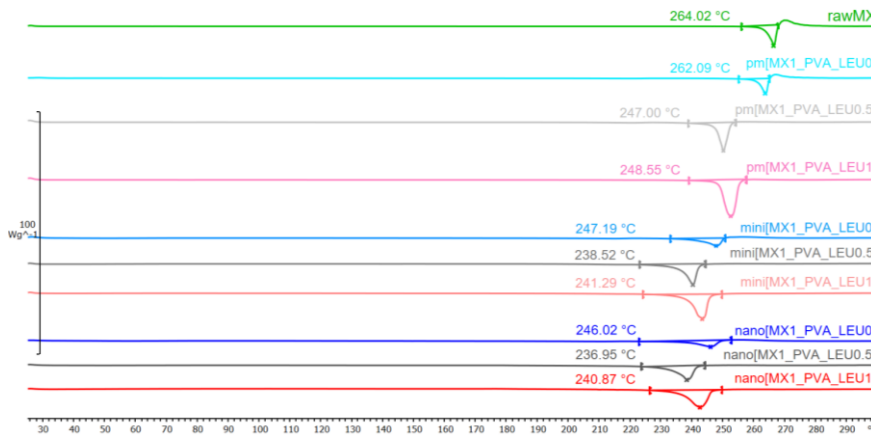


Figure 3. DSC curves of the initial MX, PM and SPD samples.

8.4.2. Findings of the crystalline structure investigation

XRPD was used to characterize the crystalline state of MX before and after the preparation process. The XRPD pattern of the raw material demonstrated the crystalline structure of MX. In the case of the products, the intensities of the characteristic peaks decreased (Figure 4.). After treatment, 73.23 % of the MX remained crystalline of the mini[MX1_PVA_LEU0], 51.81 % of the mini[MX1_PVA_LEU0.5] and 54.14 % of the mini[MX1_PVA_LEU01]. In nano[MX1_PVA_LEU0], nano[MX1_PVA_LEU0.5] and nano[MX1_PVA_LEU1] 68.19 %, 66.11% and 54.04 % of MX became amorphous.

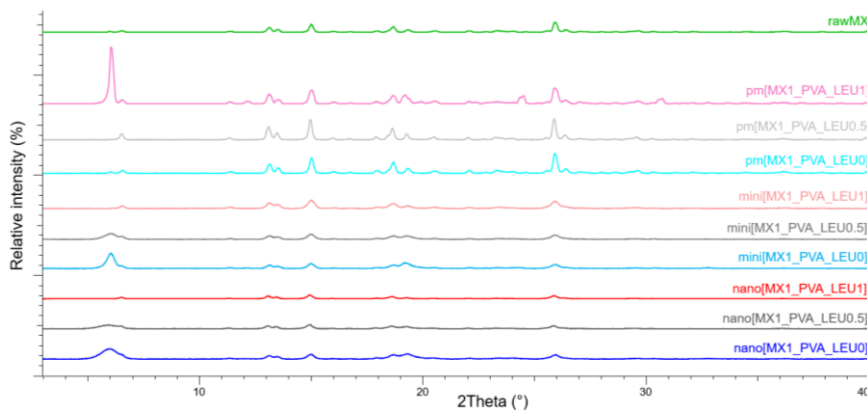


Figure 4. XRPD curves of the initial MX, PM and SPD samples.

8.5. Evaluation of the *in vitro* and *in silico* aerodynamic tests

8.5.1. Outcomes of the Andersen cascade impactor measurement

The *in vitro* aerodynamic investigation was carried out at different flow rates. The results evaluated by the Inhalytix™ software are presented in Table 5. The MMAD values of the mini SPD samples were between 3.0-3.7 μm , which were appropriate to target the smaller conducting airways. The nano SPD samples containing LEU showed MMAD between 1.2 and 1.3 μm , which was preferable to reach the deeper parts of the airways. There were MMADs smaller than 1 μm , which predicted the disintegration of the “nano-in-micro” formulations during inhalation. In the case of the LEU containing mini SPD samples, improved FPF values (up to 65%) were observed at both flow rates, indicating adequate drug delivery to patients with different lung conditions. The FPF values exceeded the commercially available DPI formulations in the Breezhaler® device. The nano SPD samples had FPF results between 87 and 95%, which was outstanding even in comparison to the formulations that are currently under development in the literature. The EF values of the LEU containing samples were also larger, especially in the case of nano SPD samples, owing to the reduced cohesion between the particles. The results of ACI are promising, due to the currently available experimental data of inhalable nanoparticles suggesting a good correlation between *in vitro* cascade impactor measurements and clinical lung deposition.

Table 5. MMAD, FPF and EF of the DPIs at a flow rate of 28.3 and 60 l/min).

Sample name	MMAD (μm)		FPF (%)		EF (%)	
	28.3 l/min	60 l/min	28.3 l/min	60 l/min	28.3 l/min	60 l/min
mini[MX1_PVA_LEU0]	3.63	3.06	68.82	54.27	72.42	53.68
	± 0.15	± 0.62	± 5.15	± 14.41	± 3.05	± 15.68
mini[MX1_PVA_LEU0.5]	3.33	0.88	65.20	72.16	83.47	61.48
	± 0.35	± 0.51	± 4.84	± 3.50	± 1.33	± 16.16
mini[MX1_PVA_LEU1]	3.37	0.91	67.03	72.26	75.22	66.28
	± 0.03	± 0.40	± 0.32	± 2.57	± 1.75	± 12.25
nano[MX1_PVA_LEU0]	4.46	2.17	21.97	62.62	54.80	28.02
	± 0.65	± 0.13	± 4.98	± 0.20	± 0.46	± 1.48
nano[MX1_PVA_LEU0.5]	0.51	1.34 \pm	69.55	86.16	61.99	54.29
	± 0.17	0.23	± 4.29	± 2.33	± 2.48	± 9.36
nano[MX1_PVA_LEU1]	0.33	1.27	82.93	94.45 \pm	73.89	92.42
	± 0.06	± 0.07	± 1.61	0.88	± 2.86	± 13.07

8.5.2. Findings of the *in silico* aerodynamic characterization

During the *in silico* characterization of the deposited and exhaled fractions of the samples were determined (Table 6. and Table 7.). Extrathoracic deposition is lower for the LEU containing products, especially in the case of nano SPD samples, due to improved

dispersity. Using a breath holding time of 10 s, the deposition in the upper airways and the exhaled fraction decreased; therefore, the bronchial and acinar deposition improved in all cases. It was shown that the length of the breath holding had a significant impact on the deposited fraction, which is not taken into account during *in vitro* aerodynamic evaluation. Larger deposition values were obtained in the lungs in the case of mini SPD samples, and the exhaled fraction was larger in the case of the nano SPD samples. However, a longer breath holding time decrease this exhaled fraction, therefore improving the deposition in smaller airways. Teaching the patients proper inhalation and breath holding techniques could improve the efficiency of the DPI and reach the smaller airways, as predicted by the ACI measurements. Several commercially available DPIs were reported to have been tested with the stochastic lung model, demonstrating less sufficient deposition compared to the presented “nano-in-micro” DPI formulations.

Table 6. *In silico* aerodynamic results at a flow rate of 28.3 l/min at a breath holding time of 5 and 10 s.

Sample name	Extrathor. (%)		Bronchial (%)		Acinar (%)		Exhaled (%)	
	5 s	10 s						
mini[MX1_PVA_LEU0]	20.75 ±1.93	20.57 ±1.93	14.54 ±0.98	15.39 ±1.00	33.65 ±2.42	35.71 ±2.40	10.48 ±0.31	7.71 ±0.26
mini[MX1_PVA_LEU0.5]	22.01 ±2.30	21.86 ±2.29	14.10 ±0.85	14.69 ±0.91	32.06 ±0.94	35.06 ±1.49	18.17 ±3.43	14.72 ±2.94
mini[MX1_PVA_LEU1]	18.82 ±0.95	18.66 ±0.95	14.32 ±0.30	14.88 ±0.31	32.65 ±0.94	36.01 ±1.03	20.25 ±0.55	16.48 ±0.44
nano[MX1_PVA_LEU0]	29.99 ±2.31	29.92 ±2.31	10.50 ±0.48	10.77 ±0.44	10.71 ±1.61	11.42 ±1.72	3.59 ±0.72	2.69 ±0.56
nano[MX1_PVA_LEU0.5]	6.64 ±0.23	6.54 ±0.22	6.15 ±0.06	6.39 ±0.12	25.93 ±0.61	30.30 ±0.96	23.24 ±2.16	18.75 ±1.86
nano[MX1_PVA_LEU1]	4.61 ±0.28	4.51 ±0.27	6.13 ±0.40	6.33 ±0.46	31.46 ±1.56	37.20 ±1.64	31.67 ±0.62	25.85 ±0.49

Table 7. *In silico* aerodynamic results at a flow rate of 60 l/min at a breath holding time of 5 and 10 s.

Sample name	Extrathor. (%)		Bronchial (%)		Acinar (%)		Exhaled (%)	
	5 s	10 s						
mini[MX1_PVA_LEU0]	34.98 ±8.09	34.53 ±8.09	10.39 ±0.05	10.39 ±0.05	9.85 ±1.76	12.80 ±2.24	23.32 ±7.35	20.68 ±6.79
mini[MX1_PVA_LEU0.5]	20.36 ±2.49	20.02 ±2.48	7.99 ±1.23	7.99 ±1.23	13.98 ±2.73	17.84 ±3.47	33.11 ±6.02	29.54 ±5.35
mini[MX1_PVA_LEU1]	22.02 ±2.62	21.56 ±2.58	9.97 ±0.65	9.97 ±0.65	16.40 ±0.81	20.92 ±1.04	37.54 ±0.82	33.46 ±0.67
nano[MX1_PVA_LEU0]	16.41 ±0.44	16.18 ±0.43	6.15 ±0.04	6.15 ±0.04	7.16 ±0.12	9.09 ±0.13	21.49 ±0.94	19.65 ±0.92
nano[MX1_PVA_LEU0.5]	7.73 ±2.06	7.57 ±2.04	5.69 ±0.52	5.69 ±0.52	13.69 ±2.56	17.11 ±3.23	45.69 ±4.17	42.18 ±3.53
nano[MX1_PVA_LEU1]	6.06 ±0.48	5.90 ±0.47	6.16 ±0.25	6.16 ±0.25	18.18 ±0.98	22.81 ±1.22	57.49 ±1.52	52.74 ±1.29

8.6. Results of the *in vitro* investigations of the pulmonary dosage form

8.6.1. Conclusion of the *in vitro* dissolution test

During the *in vitro* drug release test, the released amount of MX was the lowest for samples containing raw materials (Figure 5.). Approximately half of the drug was released from the mini SPD samples within the first 5 min compared to 5% from the reference samples. In the case of the nano SPD DPIs, in the first 5 min, up to 70% of the MX was released from the LEU containing samples, due to the smaller particle size and faster disintegration. These improvements are related to the higher specific surface area, enhanced solubility and amorphization of the MX. Hydrophilic PVA inhibited aggregation and increased polarity, LEU reduced the cohesion between the particles; therefore, a larger amount of MX was liberated. The results are beneficial in local therapy, because it gives enough time to release the nanosized MX.

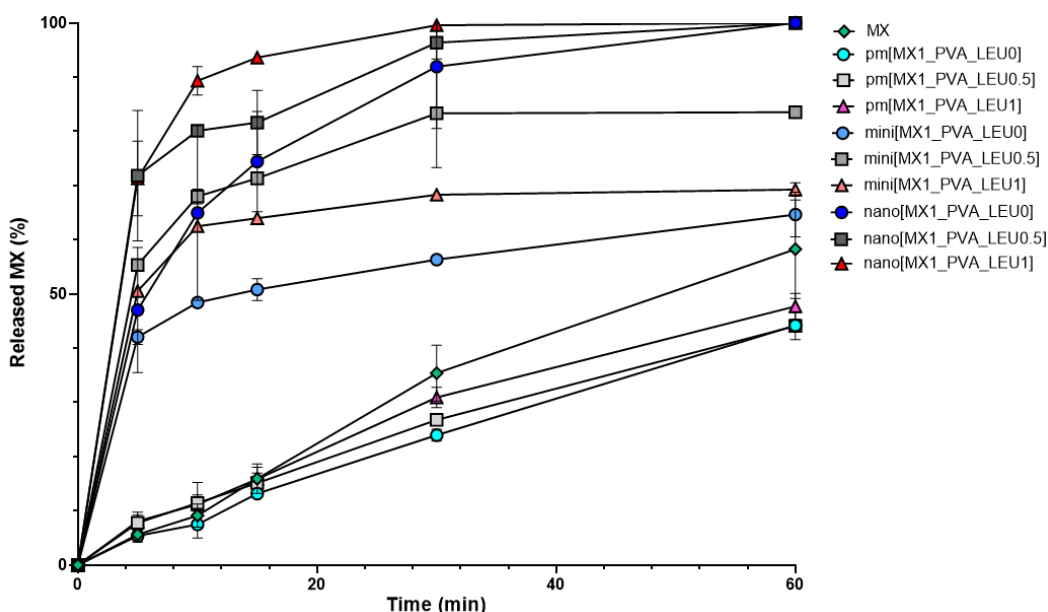


Figure 5. *In vitro* dissolution results of the DPIs containing the pulmonary dose of MX.

8.6.2. Results of the *in vitro* permeability test

During the *in vitro* diffusion study, the high surface area achieved by the nanosized particles was the main factor that influenced the rate of passive diffusion. Diffusion of the API from the samples was larger in comparison to raw MX in all samples. The K_p values of the formulations significantly improved (0.37-0.65 cm/h). The products showed significantly increased J values (Figure 6.), compared to the PMs. The results were a remarkably high amount (60–110 $\mu\text{g}/\text{cm}^2$) if we take into account that the total surface of the lung is around 100 m^2 . In overall, an increased amount of API could enter the epithelium using the SPD formulations.

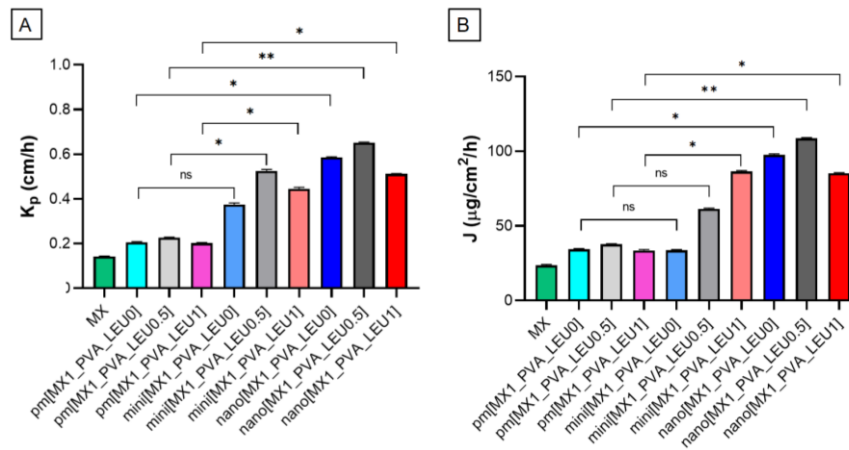


Figure 6. The results of the investigation of permeability. A: K_p results. B: J results.

8.6.3. Consequences of the *in vitro* cell line investigations

The cytotoxicity test showed that all substances have a low cytotoxic effect at a concentration of 0.1 mg/ml. Cell viability was in order to MX, nano[MX1_PVA_LEU0], nano[MX1_PVA_LEU0.5], nano[MX1_PVA_LEU1] 91.97%, 90.32%, 80.38%, and 82.77%. It can be concluded that the formulations are safe to administer pulmonary. MX containing samples inhibited IL-6 production on the translational level but not on the transcriptional level. LPS was used to increase IL-6 production in A549 cells. LPS treated cells showed significantly higher relative expression compared to untreated cells; however, neither MX nor SPD formulation inhibited the increase of IL-6 (Figure 7.). Consequently, the level of IL-6 was checked *via* ELISA, and it was found that the expression of IL-6 increased significantly in cells treated with LPS compared to cells untreated. Interestingly, MX and all SPD samples impeded IL-6 production (Figure 7.). An increase in IL-6 concentration corresponds to respiratory failure and mortality in coronavirus disease of 2019 (COVID-19), and its early reduction is promising for prolonged survival.

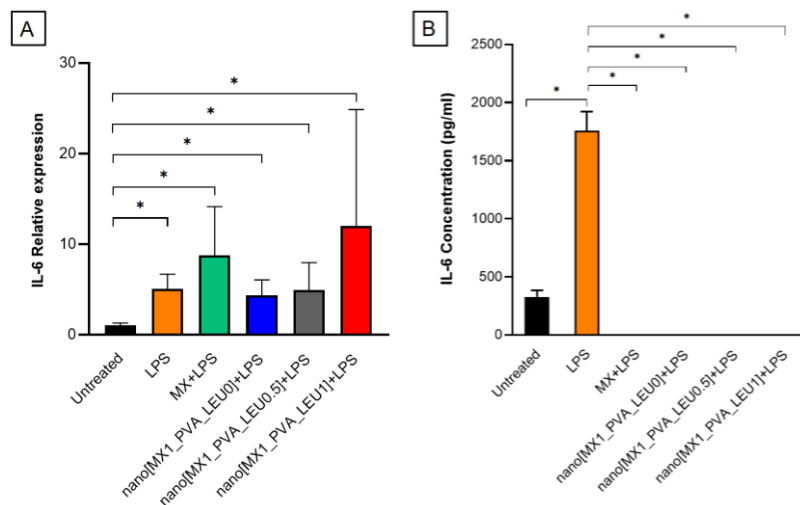


Figure 7. A: Relative expression of IL-6. A549 cells. B: Concentration of IL-6 in cell supernatants.

8.7. Results of the stability test

For the stability test, we had chosen the most promising nano[MX1_PVA_LEU1]. As reported by the characterization, the developed DPI maintained its quality attributes for an extended period. However, further stability investigations could be required, such as a test in the final package.

9. Conclusions

The purpose of the Ph.D. thesis was to develop an innovative, carrier-free “nano-in-micro” DPI system, that combines the advantages of the presence of nanosized API and the pulmonary drug delivery route. In addition to the organic-solvent free, combined preparation technique, a comprehensive investigation protocol for DPIs was developed. In line with the objectives of this dissertation, the following conclusions can be drawn:

- I. Based on a review of the literature, we pioneered the development of carrier-free “nano-in-micro” DPI formulations containing MX. To date, only a few studies have addressed the preparation of NSAID-containing DPI, and none of them have discussed the pulmonary applicability of nanosized MX. As excipients, the combination of PVA and LEU was investigated for the first time with nanosized drug to achieve adequate lung deposition without the use of other additives.
- II. The nanosuspension was prepared using an organic solvent-free wet milling method in a planetary ball mill. The optimized process resulted in a monodisperse PSD and particle size of MX below 150 nm ($D[0.5] = 137.70 \pm 4.97$ nm according to laser diffraction and $D[0.5] = 124.90 \pm 8.60$ nm according to NTA). The particle size and composition of the final suspension were suitable for further processing to create powders with a “nano-in-micro” structure.
- III. The nanosuspension was converted into a solid form by using two spray drying devices operating on different principles. It was found that both devices are capable of producing inhalation powders with suitable properties for pulmonary delivery, characterized by spherical shape and low density (0.2-0.3 g/cm³). The result of the mini spray drying was a “nano-in-micro” DPI, with particle size in the 3–4 μm range to target the bronchiolar part of the airways. Nano spray drier was utilized to create extra-fine particles smaller than 2 μm to reach the alveolar region of the lungs. The main differences between the two drying devices were in the yield, the particle size achieved and consequently the deposition pattern. The yield of spray drying

methods should be further improved in the future, especially in terms of scale-up. The incorporation of PVA contributed to the manufacture of a stable nanosuspension. It also preserved the individuality of the MX particles in their solid state. LEU enhanced the dispersibility of the powder mixture and modified the morphology of the particles, which was supported by the results of different particle size studies and SEM images. The *in vitro* and *in silico* aerodynamic characterizations demonstrated that the aerodynamic properties of the samples could be favorably influenced by appropriate LEU concentrations. *In vitro* drug release and permeability were improved by reducing interparticle cohesion.

- IV. The outstanding lung deposition of the products (FPF = $72.26 \pm 2.57\%$ of mini[MX1_PVA_LEU1] and $94.45 \pm 0.88\%$ of nano[MX1_PVA_LEU1]) was demonstrated by different aerodynamic measurements. The results of the various investigation techniques confirmed the appropriate particle size of the DPI systems to target different regions of the lung for pulmonary delivery. The mini SPD samples showed an aerodynamic diameter between 3 and 4 μm . The particle size of the nano SPD LEU containing samples were under 2 μm . The *in silico* investigation demonstrated the proper particle deposition in the bronchial (mini SPD DPI systems) and the acinar regions (nano SPD DPI systems). The prolonged breath holding time decreased the amount of API deposited in the extrathoracic areas and in the exhaled fraction.
- V. Based on the *in vitro* drug release study (between 70% and 100% of the pulmonary dose of MX in 30 min) and the *in vitro* permeability study (MX between 60-110 $\mu\text{g}/\text{cm}^2$ in 60 min), it was concluded that the formulations are suitable for pulmonary delivery. Due to the larger surface area, amorphization and the additives, dissolution was rapid in the artificial lung medium and the *in vitro* permeability of the DPIs was improved. We confirmed that the concentrations of the products applied in the lung were not toxic in A549 cell lines used to model human alveolar epithelium. According to the *in vitro* cell line test, formulations can assert a potent effect on the reduction of general inflammation by decreasing the concentration of IL-6.
- VI. The stability of a “nano-in-micro” system is crucial for future product development. It can be reported that the nano[MX1_PVA_LEU1] formulation was stable, showing no significant changes in its critical parameters for pulmonary application after 6 and 12 months.

10. Novelty and practical relevance of the work

The new findings and practical aspects of the work are summarized as follows.

- A novel “spray drying from nanosuspension” technology was developed to design MX containing “nano-in-micro” DPIs, offering the benefits of a green manufacturing process and based on literature the possibility of scale-up.
- The DPIs presented are the first in the literature to contain nanosized MX.
- The effect of combining PVA and LEU without other excipients was investigated for the first time for “nano-in-micro” DPI systems.
- A detailed investigation protocol was developed to test “nano-in-micro” DPIs including particle size analysis, drug release tests, and aerodynamic assessments, which could form the basis for the development of other DPI systems in the future.
- The formulations containing nanosized MX created by different spray drying methods exhibited excellent aerodynamic properties and better *in vitro* and *in silico* aerodynamic behavior than currently commercially available products.
- The “nano-in-micro” systems have been shown to be safe and effective according to cell line investigations and to have long-term stability.
- The novel MX containing “nano-in-micro” DPIs may offer new opportunities for the use of NSAIDs in inhalation therapy for the effective local treatment of diseases with pulmonary inflammation, such as pulmonary fibrosis, COPD, NSCLC and pneumonia caused by COVID-19 and it would be efficient for patients with weak breathing parameters.
- The preparation method could be beneficial for improving the bioavailability of other drugs with poorly water-solubility, to expand the range of the treatable lung diseases (e.g. asthma, tuberculosis).

PUBLICATIONS RELATED TO THE SUBJECT OF THE THESIS

- I. **Party, P.**; Bartos, Cs.; Farkas, Á.; Szabó-Révész, P.; Ambrus, R.; Formulation and In Vitro and In Silico Characterization of “Nano-in-Micro” Dry Powder Inhalers Containing Meloxicam, *Pharmaceutics*, 13:2, Paper: 211, 18 p. 2021.
(Q1, IF: 6.52)
- II. **Party, P.**; Kókai, D.; Burián, K.; Nagy, A.; Hopp, B.; Ambrus, R.; Development of extra-fine particles containing nanosized meloxicam for deep pulmonary delivery: in vitro aerodynamic and cell line measurements, *European Journal of Pharmaceutical Sciences*, 176, Paper: 106247, 13 p. 2022.
(Q1, IF: 4.6)
- III. **Party, P.**; Ambrus, R.; Investigation of Physico-Chemical Stability and Aerodynamic Properties of Novel “Nano-in-Micro” Structured Dry Powder Inhaler System, *Micromachines*, 14:7, Paper: 1348, 14 p. 2023.
(Q2, IF: 3.4)

PUBLICATIONS NOT RELATED TO THE SUBJECT OF THE THESIS

- I. Chvatal, A.; **Party, P.**; Katona, G.; Jójárt-Laczkovich, O.; Szabó-Révész, P.; Fattal, E.; Tsapis, N.; Ambrus, R.; Formulation and comparison of spray dried non-porous and large porous particles containing meloxicam for pulmonary drug delivery, *International Journal of Pharmaceutics*, 559 pp. 68-75., 8 p. .2019.
(D1, IF: 4.845)
- II. Party, P.; Klement, ML.; Szabó-Révész, P.; Ambrus, R.; Preparation and Characterization of Ibuprofen Containing Nano-Embedded-Microparticles for Pulmonary Delivery *Pharmaceutics*, 15:2, Paper: 545, 15 p. 2023.
(Q1; IF: 5.4)

Acknowledgement

Firstly, I would like to express my gratitude to my supervisor, **Dr. Rita Ambrus**, for all of her professional and emotional support, encouragement, and guidance.

I would like to sincerely thank **Prof. Dr. Ildikó Csóka**, Head of the Institute of Pharmaceutical Technology and Regulatory Affairs, for providing me the opportunity to work in this department and finish my doctoral research.

Also, I would like to thank **Prof. Dr. Piroska Szabó-Révész** for her scientific mentoring and **Dr. Anita Chvatal** for introducing me to the field of research as a student.

I am also grateful to my co-authors for their cooperation and invaluable help: **Dr. Csilla Balla-Bartos** from Institute of Pharmaceutical Technology and Regulatory Affairs, University of Szeged; **Dr. Árpád Farkas** from Centre for Energy Research Hungarian Academy of Sciences, **Dr. Dávid Kókai** and **Prof. Dr. Katalin Burián** from Department of Medical Microbiology, University of Szeged; **Prof. Dr. Béla Hopp** from Department of Optics and Quantum Electronics, University of Szeged; **Dr. Attila Nagy** from Wigner Research Centre for Physics, Hungarian Academy of Science.

I express appreciation to Erika Feczkoné Boda and Piroska Lakatosné Fekete for their outstanding technical help and to the undergraduate research students with whom I have worked. In addition, I would like to thank all members of the Institute of Pharmaceutical Technology and Regulatory Affairs for their help and kindness. I feel very fortunate to be able to work in such a collaborative environment.

I am thankful for my friends who supported me during the Ph.D. work: Fanni Falusi, Dorottya Németh, Szonja Plesz, Zsanett Pomaházi and Bence Sipos. I am grateful to my beloved parents, sister, niece and grandmother for their love and understanding throughout my studies. Finally, I would like to express my gratitude to Bálint Lőrinczi.

I acknowledge that the current thesis and other non-related projects were financially supported by Gedeon Richter's Talentum Foundation, Gedeon Richter Ltd., the ÚNKP-19-2-SZTE-101; ÚNKP-21-3-SZTE-258, ÚNKP-22-3-SZTE-157 and UNKP-23-3-SZTE-184 New National Excellence Program of the Ministry for Culture and Innovation from the source of the National Research, Development and Innovation Fund and by Project no. TKP2021-EGA-32 implemented with the support provided by the Ministry of Innovation and Technology of Hungary from the National Research, Development and Innovation Fund, financed under the TKP2021-EGA funding scheme and OTKA K_146148 project.